Environmental Science Nano

ROYAL SOCIETY OF CHEMISTRY

COMMUNICATION

View Article Online
View Journal | View Issue

Cite this: *Environ. Sci.: Nano*, 2025, **12**, 1821

Received 8th October 2024,
Accepted 18th January 2025

DOI: 10.1039/d4en00948g

rsc.li/es-nano

Correlation between the stability and toxicity of PFAS–nanoplastic colloids†

Katalin Viktória Bere,‡[a] Zsolt Csenki-Bakos,‡[b] Edit Kaszab,[c] Béla Urbányi,[d] István Szabó*[b] and Istvan Szilagyi *[a]

The interaction between per- and polyfluoroalkyl substances (PFASs) and nanoplastics (NPLs) in the environment is a growing concern due to their possible combined toxicity and potential impacts on ecosystems and human health. In aqueous compartments, their common migration strongly depends on the colloidal stability of the particles. Here, a clear relation between the toxicity and aggregation stage of colloids containing positively charged polystyrene NPLs and PFAS perfluorohexanoic acid (PFHxA) was established. PFHxA adsorption on NPLs altered the particle charge leading to unstable dispersions at the charge neutralization point and stable ones away from this condition. Toxicity studies on zebrafish embryos shed light on the synergistic mortality effect of the NPL–PFHxA adducts, and such a synergy strengthened with the increase in the dispersion stability highlighting the importance of environmental conditions like the NPL-to-PFAS ratio. The findings unambiguously demonstrate that high colloidal stability of environmental samples polluted with both NPLs and PFAS leads to remarkable synergistic toxicity on living ecosystems, while the individual particles are expected to migrate faster in the environment than their aggregated counterparts.

Environmental significance

The combined impact of NPLs and PFASs on the environment is particularly concerning due to their persistence, potential for bioaccumulation, and complex interactions. The present work is critical to advancing environmental science by deepening the understanding of the joint environmental behavior of these emerging pollutants, which pose significant risk on ecosystem health. By investigating the correlation between colloidal stability and associated toxicities of NPL–PFAS adducts, this research illuminates interfacial behavior at the nanoscale and its subsequent influence on mortality of model animals. The key finding of this study is that PFAS adsorption on NPL particles leads to synergistic toxic effects and such a synergy is more pronounced in stable, non-aggregating NPL–PFAS colloids. The outcome can be used during the development of regulatory policies and remediation strategies, ultimately helping to mitigate the ecological and human health risks jointly posed by these pervasive contaminants in aquatic environments.

1. Introduction

Nano and micron-sized plastic particles as well as per- and polyfluoroalkyl substances (PFASs) are two of the most notable emerging contaminants present in the environment.[1,2] Nanoplastics (NPLs) are typically smaller than 1 micrometer in size and unintentionally produced as by-products of industrial processes or from the degradation of larger plastic objects.[3–5] They exhibit colloidal behavior and thus, can rapidly spread in aqueous environments.[6] PFASs are a class of synthetic chemicals used in various industrial and consumer products, and extremely resistant to degradation processes and hazardous for all living creatures on earth.[7–9]

The interaction between plastic pollutant particles and PFASs can significantly influence their fate, transport, and potential toxicity in aquatic ecosystems.[10,11] The adsorption of PFAS onto larger plastic particles has been confirmed in several studies,[12,13] while much less information is available for NPL systems. For instance, it was found that increasing the alkyl chain length of PFASs significantly increases their affinity to NPL particles and such an adsorption process affects the stability of the dispersions.[14] Beside adsorption, the colloidal stability of plastic–PFAS aqueous systems is also influenced by the presence of dissolved electrolytes in the sample.[15] Colloid chemistry theories predict that charge

[a] *MTA-SZTE Momentum Biocolloids Research Group, Department of Physical Chemistry and Materials Science, Interdisciplinary Centre of Excellence, University of Szeged, 6720 Szeged, Hungary. E-mail: szistvan@chem.u-szeged.hu*
[b] *Department of Environmental Toxicology, Institute of Aquaculture and Environmental Safety, Hungarian University of Agriculture and Life Sciences, 2100 Gödöllő, Hungary. E-mail: szabo.istvan.temi@uni-mate.hu*
[c] *Department of Environmental Safety, Institute of Aquaculture and Environmental Safety, Hungarian University of Agriculture and Life Sciences, 2100 Gödöllő, Hungary*
[d] *Department of Aquaculture, Institute of Aquaculture and Environmental Safety, Hungarian University of Agriculture and Life Sciences, 2100 Gödöllő, Hungary*
† Electronic supplementary information (ESI) available. See DOI: https://doi.org/10.1039/d4en00948g
‡ Co-first authors.

neutralization upon PFAS adsorption induces particle aggregation and subsequent accumulation at the air–water interface or in the sediment, while charged plastic–PFAS adducts rapidly spread as individual particles in aqueous compartments.[16,17] Hence, it is obvious that the colloidal stability of such particles can have significant implications for their transport in waters and thus, their effect on living organisms and ecosystems is foreseen.

Although no direct evidence was reported for the relation between particle aggregation and toxicity, recent studies shed light on the joint harmful effects of plastic particles and PFASs. Accordingly, NPLs can increase the bioavailability of PFAS molecules through adsorption, leading to enhanced combined toxicity and increase of carcinogenic risk of PFAS by facilitating their entry into cells.[18] Besides, NPLs and PFASs have been found to have higher binding affinities to critical proteins like secretory immunoglobulin compared to control compounds.[19] Studies on aquatic organisms like shellfish, algae, and fish have shown toxicity to NPLs and PFASs, both individually and in combination.[20] Nevertheless, the state of PFAS adsorption on NPLs and its effect on the particle stability has never been related with any health effects in combined physicochemical and toxicology studies on NPL–PFAS dispersions.

The present work fills this gap, as it is concerned with the systematic evaluation of the colloidal stability and toxicity of polystyrene NPLs and PFAS perfluorohexanoic acid (PFHxA, also known as undecafluorohexanoic acid). Polystyrene is one of the most abundant NPLs in nature,[21] while PFHxA contains a C6 fluoroalkyl chain, a potential replacement of the highly toxic C8 PFAS derivatives, and it has already been detected in the environment.[22] Surface charge characteristics and particle aggregation were studied with scattering techniques and the toxicity of the systems was evaluated using zebrafish embryos. Accordingly, the main goal of this contribution is to report on the stability of colloids containing both NPLs and PFHxA and study their toxicity; in particular, a clear relation between the aggregation rate and synergistic mortality data is established for the first time.

2. Materials and methods

2.1. Materials

The sources and purity data of commercial chemicals are detailed in the ESI.† Polystyrene NPLs were synthesized by an established protocol,[23] as described in the ESI.†

2.2. NPL characterization methods

The electrophoretic mobility and hydrodynamic radius of NPLs was measured in electrophoretic (ELS) and dynamic (DLS) light scattering measurements with a Litesizer 500 (Anton Paar) and an ALV/CGS-3 compact goniometer system (ALV GmbH), respectively. The colloidal stability of the samples was expressed in terms of stability ratio (eqn (S5)†).[16] The successful formation and structure of the NPLs were explored with transmission electron microscopy (TEM, TECNAI G2 20 X-TWIN microscope) and Raman spectroscopy (Bruker Senterra II Raman microscope) in a dried state. Further details on instruments, protocols and sample preparation applied are given in the ESI.†

2.3. Assessment of embryotoxic effects

Wild-type (AB) zebrafish embryos were used for the toxicological tests. For the individual substance treatments, the embryos were exposed to the NPLs and PFHxA in different concentrations. Mortality for embryos were determined daily until 120 hpf (hours post fertilization) and lethal concentration (LC) values were calculated every day from the mortality percentages. Mortality values and sublethal effects of the treatments were determined after 120 hours of exposure. The combined influence of NPLs and PFHxA was analyzed using the combination index (CI) method based on the mortality results.[24] Further details on the experiments and CI calculations are given in the ESI.†

3. Results and discussion

3.1. NPL characterization

To explore the composition of the NPLs, their Raman spectrum was recorded (Fig. S1 in the ESI†) and the peaks were assigned to characteristic vibrations (Table S1†) of the polystyrene structure[25,26] confirming the successful preparation of the NPLs.

TEM pictures were recorded to investigate the shape and size of the NPLs in a dried state and spherical particles with some polydispersity were observed (Fig. 1a). The analysis of the images resulted in an average radius of 82.9 ± 22.4 nm. Based on DLS measurements performed in stable colloids, the mean hydrodynamic radius was determined to be 122.6 ± 12.6 nm, while the polydispersity index was 21.9 ± 14.9%. Accordingly, the prepared NPLs are rather polydisperse in size, similar to plastic particle contaminants in the environment. The DLS radius is greater than the TEM one and such a discrepancy can be explained by the stagnant hydrodynamic layer on the NPL moving together with the particle in dispersions. Thus, it contributes to the DLS measurements, but not to the TEM in dried samples leading to larger size values obtained with the former technique.[27] In addition, the higher size fraction of the NPLs contributes more to the scattering intensity and hence, shifts the average radius to larger values compared to the TEM size.

The charge of NPLs was assessed in ELS experiments (Fig. S2†). The electrophoretic mobility of the particles was positive at a low salt level and decreased with the NaCl concentration thereafter. Such a positive particle charge originates from the presence and protonation equilibrium of AIBA molecules (see section S1.2†) containing amidine groups on the NPL surface. Its value was close to zero at high salinity. The decreasing trend is due to the screening of the surface charge by the dissolved salt constituent ions, while the close to constant data at low ionic strength can be explained with the electrokinetic model.[28]

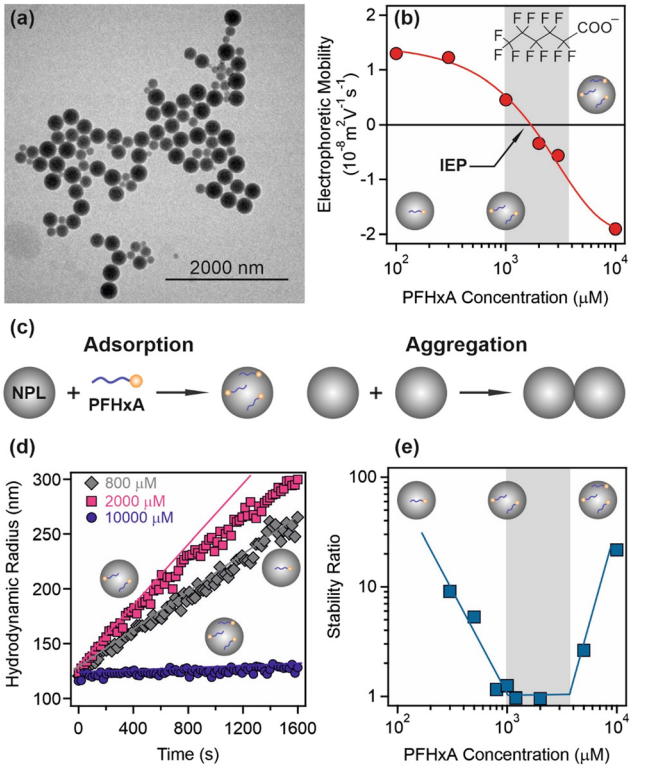

Fig. 1 TEM image of NPLs (a), electrophoretic mobility of NPLs as a function of the PFHxA concentration (b), schematic illustration of the PFHxA adsorption on the NPLs and the aggregation process (c), hydrodynamic radius *versus* time data at different PFHxA doses (d) and stability ratio values as a function of the PFHxA concentration (e). The measurements in (b), (d) and (e) were carried out at 25 mg L^{-1} NPL concentration, pH 4 and 1 mM ionic strength. The lines are eye guides in (b) and (e), while linear fits in (d) were used to calculate the apparent aggregation rate coefficients with eqn (S4).† The shaded area in (b) and (e) refers to the PFHxA concentration regime, in which rapid particle aggregation occurred.

3.2. Interaction of PFHxA with NPLs

The possible interplay between NPLs and PFHxA was explored by assessing particle aggregation and adsorption processes. Under the experimental conditions applied, the carboxylic head group of PFHxA is deprotonated due to its low pK_a value (−0.16),[29] *i.e.*, it possesses a negative charge, while the NPL surface is oppositely charged, as discussed above. Such a charge balance implies electrostatic attraction between these potential contaminants, which was studied in electrophoretic measurements (Fig. 1b).

At low PFHxA doses, the positive charge of the NPLs dominates, reflected in positive electrophoretic mobility values determined under these experimental conditions. By increasing the PFHxA dose, the mobilities decreased indicating adsorption (Fig. 1c) and consequently, charge neutralization upon the NPL–PFHxA interaction. The isoelectric point (IEP), at which the overall charge of the particle is zero, was around 2000 μM PFHxA concentration. Further increase in the PFHxA dose led to charge reversal and formation of NPL–PFHxA adducts with a negative charge. Similar charge reversal was observed with polymeric particles and surfactants.[30,31]

Time-resolved hydrodynamic radii were recorded by DLS at different PFHxA concentrations to follow possible aggregation processes under similar experimental conditions to those in the ELS study. The PFHxA dose significantly influenced the trend in the size *versus* time plots (Fig. 1d). Accordingly, particle aggregation was detected at low concentration, which accelerated at intermediate doses and slowed down at the highest PFHxA levels studied. These data were used to calculate the apparent aggregation rates (eqn (S4)†) and the stability ratios (eqn (S5)†).[15,16,30] The latter values (Fig. 1e) were high at low, close to unity at intermediate and high again at elevated PFHxA concentrations. Note that the inverse of the stability ratio gives the efficiency of the particle collisions, *i.e.*, the fraction of collisions, which results in aggregate formation. Therefore, the stability ratios close to one observed at intermediate PFHxA doses indicate rapid particle aggregation and unstable colloids, while the aggregation is slower, or not even detectable, away from this regime.

By comparing the trends observed in the electrophoretic mobility (Fig. 1b) and stability ratio (Fig. 1e) data, one can notice that the above-mentioned fast aggregation region overlaps with the PFHxA concentrations around the IEP. In other words, the surface charge of close to zero results in particle aggregation. Besides, the sufficiently large magnitudes of the mobilities at low and high PFHxA concentrations are accompanied by high stability ratios indicating the formation of more stable colloids. Such a charge–aggregation relation clearly points to the importance of the electrostatic forces between the particles and is in line with the Derjaguin–Landau–Verwey–Overbeek theory.[16,27,31] Accordingly, charged particles possess electrical double layers inducing repulsive forces upon overlap, while particles of negligible surface charge are attracted by the van der Waals forces. Hence, in the present system, the latter scenario can be applied around the IEP and the former one below and above the IEP.

These results are of particular importance in environmental water samples, in which PFAS and NPLs co-exist in different amounts. At lower and higher PFAS-to-NPL ratios, their assembly gives rise to stable colloids, which can rapidly migrate in aqueous systems and hence, transport of PFAS by NPL takes place. However, once their charge ratio is comparable, the aggregation of the formed NPL–PFAS adducts occurs. Moreover, the aggregates may interlink leading to accumulation at the water–air interface or in the sediment depending on the density of the particles and the medium. The relation of the stage of aggregation and charge of particles to their toxicity was investigated as follows.

3.3. Toxicity results of the individual substance treatments

To analyze the embryotoxic effects and to determine the concentrations to be used for co-exposure experiments, the

embryos were treated with different concentrations of NPL and PFHxA from 2 to 120 hpf (Fig. S3†). Mortality was recorded daily and LC_1, LC_{10}, LC_{25} and LC_{50} values were determined (see ESI† for experimental details). NPL toxicity was relatively low throughout the experiments (Fig. S3a†). The calculated LC_{50} value was the highest after 24 hours (760.9 mg L^{-1}), which decreased after 48 hours (442.2 mg L^{-1}). The LC_{50} data showed a slight decrease between 48 and 96 hours. The toxicity of the NPLs in the last 24 hours of the treatment increased noticeably compared to the previous periods and the LC_{50} value decreased to 135.6 mg L^{-1} (Table S2†). No mortality was detected in the control groups.

Embryonic chorions provide an optimal microenvironment for the developing embryo and are efficient barriers against exogenous pollutants including microplastics and NPLs.[32,33] The chorion has a special biological structure and comprises a large number of pores with diameters of up to 500 nm,[34] which, among others, allows the essential oxygen to pass through. Embryonic chorions exhibit high affinity to plastic particles, which gradually adhere to the surface and clog the pores.[35] As time passes, the deposition of NPLs can reach the extent to create a hypoxic environment around the developing embryo leading to developmental disorders or mortality. Under normal conditions, zebrafish embryos hatch between 48–72 hpf. After hatching, the uptake by zebrafish larvae becomes more complex, as more and more exposure ways open up to the particles. Starting from hatching, the embryo can come into contact with the particles on its entire body surface, and right before the free feeding stage (96–120 hpf), it can even consume them through the mouth.[32,36] Therefore, starting from hatching, NPLs appear in increasing proportions in some organs of the larvae (*e.g.*, gills, blood vessels, digestive tract or brain), which can cause further malformations and dysfunctions.[32,35,37] These processes may explain the drastic change in LC_{50} values observed during the NPL exposure test.

In the case of PFHxA, mild changes can be observed between the LC_{50} values by varying the loading amount (Fig. S3b†). The LC_{50} value calculated after 24 hour exposure decreased from 407.4 μM to only 368.0 μM by the end of the 120 hour exposure time (Table S2†) explained by the kinetics of the substance. The uptake rate constant of shorter chain length PFASs (linear C–F ≤ 6) like PFHxA is significantly lower than that of longer chain PFASs, while their elimination rate constant is significantly higher. This means that PFHxA is less prone to accumulate in the embryo tissues and is eliminated more easily from the embryos.[38] In the control groups, no mortality was detected.

3.4 Results of the co-exposure treatments

Besides the two fixed NPL concentrations (25 mg L^{-1} and 100 mg L^{-1}), two non-toxic PFHxA doses (100 μM and 250 μM), another two toxic concentrations in the LC_{10} and LC_{25} range (300 and 350 μM) and an amount causing 100% mortality (1000 μM) were selected for the co-exposure tests. In addition to the mortality, the combined effect of the mixtures was analyzed using the CI method.[24] The latter parameter was determined to assess possible synergistic toxicity effects of the NPL–PFHxA compounds.

In general, the combinations always caused a higher toxicity compared to the corresponding PFHxA treatments alone. A 100% mortality was caused by mixtures containing 350 μM and 1000 μM PFHxA (Fig. 2a and Table S3†). For the combinations containing 25 mg L^{-1} NPL, synergism was noticeable in all cases (CI: 0.50–0.30, see Fig. 2b). Regarding the samples with 100 mg L^{-1} NPL, the two lowest PFHxA concentrations induced an antagonistic effect (CI: 1.31 and 1.16), the 100 mg L^{-1} NPL and 350 μM PFHxA co-exposure had an additive effect (CI: 0.95), and a synergism was observed for the two highest PFHxA contents (CI: 0.78 and 0.63).

Comparing the toxicity results of the NPLs, PFAS and their combinations with the colloidal stability of the samples at 25 mg L^{-1} NPL and varying PFHxA concentrations, a clear relation can be established in the 100–1000 μM regime, which corresponds to the experimental conditions before the IEP. In these samples, both the stability ratio and CI data could be precisely determined. Individual toxicity was found neither for NPL at 25 mg L^{-1} nor for PFHxA at 100 and 250 μM concentrations. However, their mixture caused detectable mortality indicating the synergistic effect of these contaminants upon interaction. Such a synergy can be also observed at higher PFHxA concentrations and both the CI indices and the stability ratios decrease with the PFHxA loading (Fig. 2b). These observations imply that acceleration in particle aggregation leads to a decrease in the toxicity synergy. In other words, such a synergistic effect is more pronounced, when the NPL–PFHxA adducts form more stable colloids and can spread more rapidly in liquid media. Note that similar comparison at 100 mg L^{-1} NPL concentration was not possible, because of the strong multiple scattering events, which prevent the performance of accurate light scattering measurements at this high particle dose.

Furthermore, sublethal symptoms of individual treatments and co-exposures were also examined at the end of the exposure period (Fig. 3).

In general, an uninflated swim bladder appeared as the most prominent symptom, which affected 100% of the embryos in the single exposures to NPLs and PFHxA and their mixture. The 100 mg L^{-1} NPL concentration induced changes in the shape and color of the yolk, and caused pericardial edema. Discoloration of the yolk also occurred in all embryos treated with mixtures containing 100 mg L^{-1} NPL. Pericardial edema was also observed in the mixtures containing a lower particle concentration. In the individual treatments with 250 and 300 μM PFHxA, pericardial edema was observed in addition to the uninflated swim bladder. In the literature, several other malformations are mentioned in the case of plastic particles and PFAS pollutants, such as

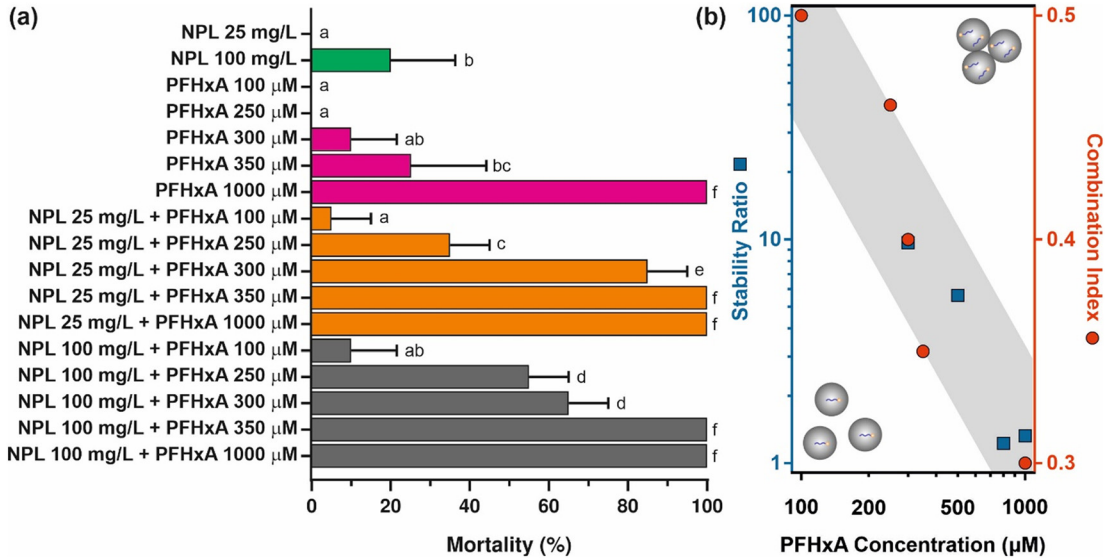

Fig. 2 Mortality caused by NPLs (25 mg L^{-1} and 100 mg L^{-1}) and PFHxA (100, 250, 300, 350 and 1000 μM) alone and in combinations after 120 hour treatment of zebrafish embryos (a). Different letters indicate significant differences in mortality data ($p < 0.05$). Stability ratios (left axis) and synergistic combination indices (right axis) determined in the NPL–PFHxA systems at 25 mg L^{-1} NPL and various PFHxA concentrations (b).

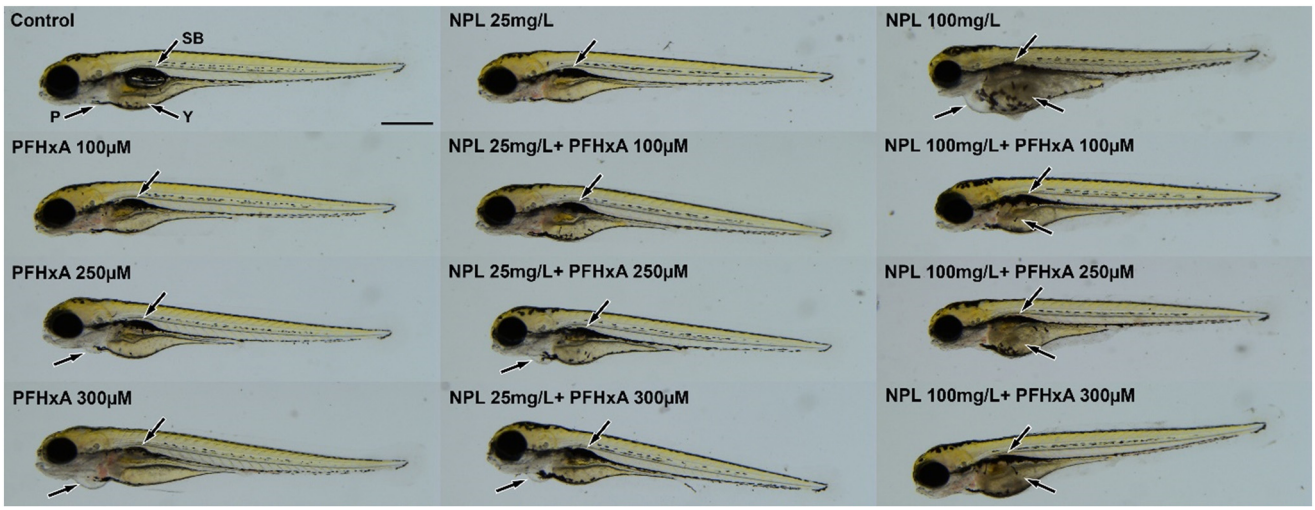

Fig. 3 Sublethal effects of NPLs (25 mg L^{-1} and 100 mg L^{-1}) and PFHxA (100, 250 and 300 μM) alone and in combinations after 120 hour treatment of zebrafish embryos. Representative phenotype lesions are indicated by arrows. P refers to pericardium, SB to swim bladder and Y to yolk. The scale bar indicates 500 μM.

higher head height, pine curvature, caudal flexure, and larger optic vesicle area.[35,37,39] For PFAS compounds, altered liver and pancreas morphology, body curvature, and tail malformations were reported.[40,41] Nevertheless, these were not detectable in our experiments.

4. Conclusions

In conclusion, the present results shed light on the importance of NPL–PFAS interactions in aqueous media. Experimental data proved that these emerging contaminants form new types of hazardous compounds upon adsorption of PFAS on NPLs, which alter the surface charge and consequently the colloidal stability of the systems. The aggregation stage of NPL–PFAS adducts not only influence the spreading and accumulation processes in water, but also leads to synergistic toxic effects depending on the NPL-to-PFAS ratio in the contaminated areas. Correlation between colloidal stability and toxicity of NPL–PFAS systems has not been reported in the past. Therefore, the present findings bring important new insights into the relation of the interfacial processes to the potential health effects in samples jointly containing emerging contaminants, as the case in many environmental water samples.

Data availability

Data for this article, including the electrophoretic mobility, hydrodynamic radius, stability ratio, Raman intensity, mortality, CI, and LC values are available at the server of the University of Szeged faculty members at **https://www.staff.u-szeged.hu/~szistvan/EnvSciNano_Bereetal**.

Conflicts of interest

The authors declare no conflicts of interest.

Acknowledgements

The support of the National Research, Development and Innovation office through proposals SNN142258 and 2024-1.2.3-HU-RIZONT-2024-00010 is gratefully acknowledged. This work was supported by the 2020-1.1.2-PIACI-KFI-2021-00239 that has been implemented with the support provided by the Ministry of Innovation and Technology of Hungary from the National Research, Development, and Innovation Fund, financed under the PIACI KFI funding scheme, by the Ministry of Innovation and Technology within the framework of the Thematic Excellence Programme 2021, National Defense and Security sub-programme (TKP2021-NVA-22) and 'PFAQuatic' 2024-1.2.3-HU-RIZONT-2024-00100 projects. This research was also financed by the Research Excellence Programme (Z. C.-B.) and the Flagship Research Groups Programme (B. U. and I. Sza.) of the Hungarian University of Agriculture and Life Sciences. The contributions of Szilárd Sáringer and Adél Szerlauth in the preparation of NPLs and the recording of the Raman spectra, respectively, are gratefully acknowledged. The authors thank the University of Szeged Open Access Fund (7467) for support.

References

1 D. M. Mitrano and M. Wagner, A sustainable future for plastics considering material safety and preserved value, *Nat. Rev. Mater.*, 2022, **7**, 71–73.
2 J. H. Fang, K. R. Xu, A. R. Liu, Y. H. Xue, L. N. Tie, Z. L. Deng, R. L. Qiu and W. X. Zhang, Selective perfluorooctanoic acid (PFOA) and perfluorooctane sulfonate (PFOS) adsorption by nanoscale zero-valent iron (nZVI): performance and mechanisms, *Environ. Sci.:Nano*, 2024, **11**, 1915–1925.
3 D. M. Mitrano, P. Wick and B. Nowack, Placing nanoplastics in the context of global plastic pollution, *Nat. Nanotechnol.*, 2021, **16**, 491–500.
4 A. Arini, S. Muller, V. Coma, E. Grau, O. Sandre and M. Baudrimont, Origin, exposure routes and xenobiotics impart nanoplastics with toxic effects on freshwater bivalves, *Environ. Sci.:Nano*, 2023, **10**, 1352–1371.
5 J. Caldwell, P. Taladriz-Blanco, L. Rodriguez-Lorenzo, B. Rothen-Rutishauser and A. Petri-Fink, Submicron- and nanoplastic detection at low micro- to nanogram concentrations using gold nanostar-based surface-enhanced Raman scattering (SERS) substrates, *Environ. Sci.:Nano*, 2024, **11**, 1000–1011.
6 O. S. Alimi, J. F. Budarz, L. M. Hernandez and N. Tufenkji, Microplastics and nanoplastics in aquatic environments: Aggregation, deposition, and enhanced contaminant transport, *Environ. Sci. Technol.*, 2018, **52**, 1704–1724.
7 S. Joudan, J. Gauthier, S. A. Mabury and C. J. Young, Aqueous leaching of ultrashort-chain PFAS from (fluoro) polymers: Targeted and nontargeted analysis, *Environ. Sci. Technol. Lett.*, 2024, **11**, 237–242.
8 H. Schwartz-Narbonne, C. J. Xia, A. Shalin, H. D. Whitehead, D. W. Yang, G. F. Peaslee, Z. Y. Wang, Y. Wu, H. Peng, A. Blum, M. Venier and M. L. Diamond, Per- and polyfluoroalkyl substances in Canadian fast food packaging, *Environ. Sci. Technol. Lett.*, 2023, **10**, 343–349.
9 F. Vahedian, J. A. K. Silva, J. Simunek and J. E. McCray, Influence of tension-driven flow on the transport of AFFF in unsaturated media, *ACS ES&T Water*, 2024, **4**, 564–574.
10 M. M. Rahman, M. B. Sultan and M. Alam, Microplastics and adsorbed micropollutants as emerging contaminants in landfill: A mini review, *Curr. Opin. Environ. Sci. Health*, 2023, **31**, 100420.
11 F. Yu, J. Wu, H. Wang, Y. Bao, H. Xing, W. Ye, X. Li and M. Huang, Interaction of microplastics with perfluoroalkyl and polyfluoroalkyl substances in water: A review of the fate, mechanisms and toxicity, *Sci. Total Environ.*, 2024, **948**, 175000.
12 J. X. Sun, H. Xiang, X. T. Jiang, X. Wang, X. Luo, J. Fu and J. X. Fan, Effects of polyamide microplastics on the adsorption of perfluoroalkyl substances in soil, *J. Hazard. Mater. Adv.*, 2024, **13**, 100391.
13 O. A. Salawu, C. I. Olivares and A. S. Adeleye, Adsorption of PFAS onto secondary microplastics: A mechanistic study, *J. Hazard. Mater.*, 2024, **470**, 134185.
14 K. Bere, B. Bakk, E. Illés, M. Kocsis, A. Jamnik, M. Tomsic and I. Szilagyi, Role of fluorocarbon chain length in the adsorption of perfluoroalkyl substances on nanoplastic particles, *ACS ES&T Water*, 2024, **4**, 5114–5121.
15 K. Bere, X. Xiong, S. Sáringer, G. Douglas and I. Szilagyi, Microplastics as an adsorption and transport medium for per- and polyfluoroalkyl substances in aquatic systems: Polystyrene and undecafluorohexanoic acid interactions, *J. Mol. Liq.*, 2023, **384**, 122285.
16 M. Elimelech, J. Gregory, X. Jia and R. A. Williams, *Particle deposition and aggregation: Measurement, modeling, and simulation*, Butterworth-Heinemann Ltd., Oxford, 1995.
17 K. Mensah, A. Magdaleno, S. Yaparatne, S. Garcia-Segura and O. G. Apul, Emerging investigator series: suspended air nanobubbles in water can shuttle polystyrene nanoplastics to the air-water interface, *Environ. Sci.: Nano*, 2024, **11**, 3721–3728.
18 N. Sun, H. J. Shi, X. X. Li, C. Z. Gao and R. T. Liu, Combined toxicity of micro/nanoplastics loaded with environmental pollutants to organisms and cells: Role, effects, and mechanism, *Environ. Int.*, 2023, **171**, 107711.
19 C. E. Enyoh, P. E. Ovuoraye, W. Qingyue and W. Q. Wang, Examining the impact of nanoplastics and PFAS exposure on immune functions through inhibition of secretory

immunoglobin A in human breast milk, *J. Hazard. Mater.*, 2023, **459**, 132103.
20 Y. H. Dai, J. Zhao, C. X. Sun, D. Y. Li, X. Liu, Z. Y. Wang, T. T. Yue and B. S. Xing, Interaction and combined toxicity of microplastics and per- and polyfluoroalkyl substances in aquatic environment, *Front. Environ. Sci. Eng.*, 2022, **16**, 136.
21 T. Kogel, O. Bjoroy, B. Toto, A. M. Bienfait and M. Sanden, Micro- and nanoplastic toxicity on aquatic life: Determining factors, *Sci. Total Environ.*, 2020, **709**, 136050.
22 S. N. Zhang, X. C. Guo, S. Y. Lu, J. He, Q. Wu, X. H. Liu, Z. Y. Han and P. Xie, Perfluorohexanoic acid caused disruption of the hypothalamus-pituitary-thyroid axis in zebrafish larvae, *Ecotoxicol. Environ. Saf.*, 2022, **232**, 8.
23 D. S. Yun, H. S. Lee, H. G. Jang and J. W. Yoo, Controlling size and distribution for nano-sized polystyrene spheres, *Bull. Korean Chem. Soc.*, 2010, **31**, 1345–1348.
24 T. C. Chou, Theoretical basis, experimental design, and computerized simulation of synergism and antagonism in drug combination studies, *Pharmacol. Rev.*, 2006, **58**, 621–681.
25 A. B. D. Nandiyanto, A. Suhendi, T. Ogi, T. Iwaki and K. Okuyama, Synthesis of additive-free cationic polystyrene particles with controllable size for hollow template applications, *Colloids Surf., A*, 2012, **396**, 96–105.
26 L. Montano, E. Giorgini, V. Notarstefano, T. Notari, M. Ricciardi, M. Piscopo and O. Motta, Raman microspectroscopy evidence of microplastics in human semen, *Sci. Total Environ.*, 2023, **901**, 165922.
27 M. Schudel, S. H. Behrens, H. Holthoff, R. Kretzschmar and M. Borkovec, Absolute aggregation rate constants of hematite particles in aqueous suspensions: A comparison of two different surface morphologies, *J. Colloid Interface Sci.*, 1997, **196**, 241–253.
28 M. Borkovec, S. H. Behrens and M. Semmler, Observation of the mobility maximum predicted by the standard electrokinetic model for highly charged amidine latex particles, *Langmuir*, 2000, **16**, 5209–5212.
29 E. Gagliano, M. Sgroi, P. P. Falciglia, F. G. A. Vagliasindi and P. Roccaro, Removal of poly- and perfluoroalkyl substances (PFAS) from water by adsorption: Role of PFAS chain length, effect of organic matter and challenges in adsorbent regeneration, *Water Res.*, 2020, **171**, 115381.
30 M. Kobayashi, S. Yuki and Y. Adachi, Effect of anionic surfactants on the stability ratio and electrophoretic mobility of colloidal hematite particles, *Colloids Surf., A*, 2016, **510**, 190–197.
31 T. C. Cao, M. Borkovec and G. Trefalt, Heteroaggregation and homoaggregation of latex particles in the presence of alkyl sulfate surfactants, *Colloids Interfaces*, 2020, **4**, 52.
32 Z. H. Duan, X. Y. Duan, S. Zhao, X. L. Wang, J. Wang, Y. B. Liu, Y. W. Peng, Z. Y. Gong and L. Wang, Barrier function of zebrafish embryonic chorions against microplastics and nanoplastics and its impact on embryo development, *J. Hazard. Mater.*, 2020, **395**, 122621.
33 L. A. Kristofco, S. P. Haddad, C. K. Chambliss and B. W. Brooks, Differential uptake of and sensitivity to diphenhydramine in embryonic and larval zebrafish, *Environ. Toxicol. Chem.*, 2018, **37**, 1175–1181.
34 J. P. Cheng, E. Flahaut and S. H. Cheng, Effect of carbon nanotubes on developing zebrafish (*Danio rerio*) embryos, *Environ. Toxicol. Chem.*, 2007, **26**, 708–716.
35 L. Y. Qiang and J. P. Cheng, Exposure to microplastics decreases swimming competence in larval zebrafish (*Danio rerio*), *Ecotoxicol. Environ. Saf.*, 2019, **176**, 226–233.
36 Q. Q. Chen, M. Gundlach, S. Y. Yang, J. Jiang, M. Velki, D. Q. Yin and H. Hollert, Quantitative investigation of the mechanisms of microplastics and nanoplastics toward zebrafish larvae locomotor activity, *Sci. Total Environ.*, 2017, **584**, 1022–1031.
37 J. Bhagat, L. Q. Zang, N. Nishimura and Y. Shimada, Zebrafish: An emerging model to study microplastic and nanoplastic toxicity, *Sci. Total Environ.*, 2020, **728**, 138707.
38 W. Wen, X. H. Xia, D. Zhou, H. T. Wang, Y. W. Zhai, H. Lin, J. Chen and D. X. Hu, Bioconcentration and tissue distribution of shorter and longer chain perfluoroalkyl acids (PFAAs) in zebrafish (*Danio rerio*): Effects of perfluorinated carbon chain length and zebrafish protein content, *Environ. Pollut.*, 2019, **249**, 277–285.
39 G. Malafaia, A. M. de Souza, A. C. Pereira, S. Gonçalves, A. P. D. Araújo, R. X. Ribeiro and T. L. Rocha, Developmental toxicity in zebrafish exposed to polyethylene microplastics under static and semi-static aquatic systems, *Sci. Total Environ.*, 2020, **700**, 134867.
40 H. H. Huang, C. J. Huang, L. J. Wang, X. W. Ye, C. L. Bai, M. T. Simonich, R. L. Tanguay and Q. X. Dong, Toxicity, uptake kinetics and behavior assessment in zebrafish embryos following exposure to perfluorooctanesulphonicacid (PFOS), *Aquat. Toxicol.*, 2010, **98**, 139–147.
41 Y. Rericha, M. T. Simonich, L. Truong and R. L. Tanguay, Review of the zebrafish as a model to investigate per- and polyfluoroalkyl substance toxicity, *Toxicol. Sci.*, 2023, **194**, 138–152.